

1 **Current status of model predictions on volatile organic compounds and impacts**  
2 **on surface ozone predictions during summer in China**

3 Yongliang She<sup>1</sup>, Jingyi Li<sup>1</sup>, Xiaopu Lyu<sup>2</sup>, Hai Guo<sup>3</sup>, Momei Qin<sup>1</sup>, Xiaodong Xie<sup>1</sup>, Kangjia  
4 Gong<sup>1</sup>, Fei Ye<sup>1</sup>, Jianjiong Mao<sup>1</sup>, Lin Huang<sup>1</sup>, Jianlin Hu<sup>1\*</sup>

5  
6 <sup>1</sup> *Jiangsu Key Laboratory of Atmospheric Environment Monitoring and Pollution*  
7 *Control, Jiangsu Collaborative Innovation Center of Atmospheric Environment and*  
8 *Equipment Technology, School of Environmental Science and Engineering, Nanjing*  
9 *University of Information Science & Technology, 219 Ningliu Road, Nanjing 210044,*  
10 *China*

11 <sup>2</sup> *Department of Geography, Hong Kong Baptist University, Hong Kong 000000, China*

12 <sup>3</sup> *Department of Civil and Environmental Engineering, The Hong Kong Polytechnic*  
13 *University, Hong Kong 00000, China*

14  
15 \* Corresponding author:

16 Jianlin Hu, Email: [jianlinhu@nuist.edu.cn](mailto:jianlinhu@nuist.edu.cn).

17 **Abstract**

18 Volatile organic compounds (VOCs) play a crucial role in the formation of  
19 tropospheric ozone (O<sub>3</sub>) and secondary organic aerosols. VOC emissions are generally  
20 considered to have larger uncertainties compared to other pollutants, such as sulphur  
21 dioxide and fine particulate matter (PM<sub>2.5</sub>). Although predictions of O<sub>3</sub> and PM<sub>2.5</sub> have  
22 been extensively evaluated in air quality modelling studies, there has been limited  
23 reporting on the evaluation of VOCs, mainly due to a lack of routine VOCs  
24 measurements at multiple sites. In this study, we utilized VOCs measurements from the  
25 ATMSYC project at 28 sites across China and assessed the predicted VOCs  
26 concentrations using the Community Multiscale Air Quality (CMAQ) model with the  
27 widely used Multi-resolution Emission Inventory for China (MEIC). The ratio of  
28 predicted to observed total VOCs was found to be  $0.74 \pm 0.40$ , with underpredictions  
29 ranging from 2.05 to 50.61 ppbv (5.77% to 85.40%) at 24 sites. A greater bias in VOCs  
30 predictions was observed in industrial cities in the north and southwest, such as Jinan,  
31 Shijiazhuang, Lanzhou, Chengdu, and Guiyang. In terms of different VOC components,  
32 alkanes, alkenes, non-naphthalene aromatics (ARO2MN), alkynes and HCHO had  
33 prediction-to-observation ratios of  $0.53 \pm 0.38$ ,  $0.51 \pm 0.48$ ,  $0.31 \pm 0.38$ ,  $0.41 \pm 0.47$   
34 and  $1.21 \pm 1.61$ , respectively.~~In terms of different VOC components, alkanes, alkenes,~~  
35 ~~non-naphthalene aromatics (ARO2MN), and alkynes were consistently underpredicted,~~  
36 ~~with ratios of predicted to observed of  $0.53 \pm 0.38$ ,  $0.51 \pm 0.48$ ,  $0.31 \pm 0.38$ , and  $0.41$~~   
37  ~~$\pm 0.47$ , respectively.~~ Sensitivity experiments were conducted to assess the impact of the  
38 VOCs prediction bias on O<sub>3</sub> predictions. While emission adjustments improved the  
39 model performance for VOCs, resulting in a ratio of total VOCs to  $0.86 \pm 0.47$ , they  
40 also exacerbated O<sub>3</sub> overprediction relative to the base case by 0.62% to 6.27% across  
41 the sites. This study demonstrates that current modelling setups and emission

42 inventories are likely to underpredict VOCs concentrations, and this underprediction of  
43 VOCs contributes to lower O<sub>3</sub> predictions in China.

44 **Keywords:** *volatile organic compounds, O<sub>3</sub> prediction, model evaluation, emissions*

## 45 **1. Introduction**

46 Volatile organic compounds (VOCs) in the ambient atmosphere consist of  
47 thousands of gaseous organic trace substances emitted from various anthropogenic and  
48 biogenic sources (Guenther et al., 2012; Li et al., 2017a; Kelly et al., 2018). These  
49 compounds undergo complex chemical reactions that form ozone (O<sub>3</sub>) and secondary  
50 organic aerosols (SOA) (Sillman, 1999; Kroll and Seinfeld, 2008). While biogenic  
51 VOCs (BVOCs) are the primary source of VOCs worldwide (Guenther et al., 2006),  
52 urban areas are predominantly influenced by anthropogenic sources (Guan et al., 2020;  
53 Guo et al., 2022; Li et al., 2022a). Anthropogenic VOCs (AVOCs) emission inventories  
54 are typically developed by estimating the total VOCs emissions using emission factors  
55 (EFs) and activity rates from different sources. The VOCs speciation profiles are then  
56 utilized to determine the emission rates of various VOCs species (Li et al., 2017a). Due  
57 to the complexity of VOCs emission processes and presence of numerous small but  
58 dispersed nonpoint sources, notable uncertainties exist while determining EFs, activity  
59 rates, and speciation profiles. It is estimated that the uncertainties associated with VOCs  
60 emissions range from approximately 68% to 76%, which are higher than those of  
61 sulphur dioxide (SO<sub>2</sub>) (12% to 40%), nitrogen dioxide (NO<sub>x</sub>) (31% to 35%), and  
62 particulate matter (PM) (30% to 94%) (Zhang et al., 2009; Li et al., 2019; Kurokawa  
63 and Ohara, 2020; An et al., 2021).

64 Chemical transport models (CTMs), such as the Community Multiscale Air  
65 Quality (CMAQ) model, Weather Research and Forecasting model coupled with  
66 Chemistry (WRF-Chem), and Goddard Earth Observing System Chemical transport

67 model (GEOS-Chem) have been developed and widely used to investigate the  
68 formation processes, source apportionment, and emission control strategies for various  
69 air pollution issues (Zhang et al., 2021; Dang et al., 2021; Wang et al., 2021). The  
70 emissions of VOCs, along with other species such as SO<sub>2</sub>, NO<sub>x</sub>, ammonia, and PM,  
71 serve as essential inputs driving air quality model simulations. Uncertainties in VOCs  
72 emissions notably impact air quality modelling for O<sub>3</sub>, SOA, and total fine particulate  
73 matter (PM<sub>2.5</sub>)PM<sub>2.5</sub>. A study conducted in the United States reported a substantial  
74 underprediction of VOCs emission inventories in urban regions (McDonald et al., 2018),  
75 particularly for volatile chemical products (VCPs). A simulation study that developed  
76 four cases based on the baseline inventory demonstrated that augmented VOCs  
77 emission inventories have notable effects on O<sub>3</sub> and PM<sub>2.5</sub> air pollutants, highlighting  
78 the need for more detailed VCPs emissions in the inventory to improve enhance-model  
79 performance (Zhu et al., 2019). In China, notable discrepancies in aromatics have been  
80 observed between CMAQ predictions and measurements (Wang et al., 2020). Wu et al.  
81 (2022) reconciled the bottom-up methodology and measurement constraints to improve  
82 the city-scale non-methane VOCs (NMVOCs) emission inventory in Nanjing, resulting  
83 in improved O<sub>3</sub> simulation performance with the CMAQ model.

84 Model evaluation serves as the initial step in establishing confidence in air quality  
85 model predictions for further analysis. Numerous studies have conducted evaluations  
86 of the predicted O<sub>3</sub> and PM<sub>2.5</sub> concentrations in China (Hu et al., 2016; Li et al., 2021b;  
87 Li et al., 2020). Overall, the predictions of O<sub>3</sub> and PM<sub>2.5</sub> concentrations generally align  
88 with the observations (Shi et al., 2017; Wang et al., 2021), although substantial biases  
89 have been reported in certain circumstances and for specific species, such as O<sub>3</sub> and  
90 SOA (Gong et al., 2021; Liu et al., 2020; Hu et al., 2017; Qin et al., 2018). Given that  
91 VOCs are key precursors of O<sub>3</sub> and SOA, evaluating VOCs predictions can help

92 elucidate the causes of these substantial biases in predictions. However, VOCs  
93 evaluations in regional modelling studies have been infrequent due to limited  
94 measurement data. Ambient VOCs have been measured at different locations in China  
95 in various studies (Yang et al., 2022; Wang et al., 2022a). Unlike O<sub>3</sub> and PM<sub>2.5</sub>, which  
96 are routinely monitored across major cities and regions in China, VOCs are often  
97 measured over short periods at one or specific sites. Different studies may employ  
98 different instruments and the study periods may vary, making it challenging to compile  
99 VOCs measurement data from multiple studies for a comprehensive model evaluation.

100 In this study, we conducted VOCs evaluations ~~for the first time~~ in China by  
101 utilizing summertime observations from 28 sites located in different regions of the  
102 country, as part of the "Towards an Air Toxic Management System in China  
103 (ATMSYC)" project (Lyu et al., 2020). This study aimed to assess the disparities  
104 between measured VOC concentrations and predictions in various regions of China  
105 using the widely used CMAQ model. We quantified the impacts of VOC biases on O<sub>3</sub>  
106 predictions through emission adjustments based on observation-prediction differences.  
107 ~~This study aimed to: (1) assess the disparities in VOC levels between measured ambient~~  
108 ~~concentrations and predicted concentrations in various regions of China using the~~  
109 ~~widely used CMAQ model, (2) quantify the impacts of VOCs species with substantial~~  
110 ~~biases on O<sub>3</sub> predictions through emission adjustments based on observation-prediction~~  
111 ~~differences, and (3) evaluate the sensitivity of O<sub>3</sub> formation to VOCs in key cities,~~  
112 ~~providing recommendations on the necessity of emission inventories and pollution~~  
113 ~~control measures. The results of this study indicated that the model performance of~~  
114 VOCs in China still has much room to improve, likely with a focus on updating  
115 emission inventories in fast-growing industrial cities. Most sites underpredicted  
116 TVOCs, and the biases of alkenes significantly impacted O<sub>3</sub> production. These findings

117 enhanced our understanding of the current VOC modelling in air quality models, which  
118 could help to improve VOC emission inventory and O<sub>3</sub> prediction in the future.

## 119 **2. Materials and Methods**

### 120 2.1. Observation ~~description~~data

121 The ATMSYC project involved a collaborative sampling campaign at 28 sites in 18  
122 cities across China, conducted from 6 June to 24 August, 2018, with speciated VOC  
123 measurements as part of the observation task (Lyu et al., 2020). Detailed site  
124 information and sampling times can be found in Table S1. Measurements were taken at  
125 intervals of two or four hours between 8:00 and 16:00. The offline measurement  
126 techniques, and data quality assurance and quality controls (QA/QC), which were  
127 consistent across all sites, have been previously described (Lyu et al., 2019; Lyu et al.,  
128 2020; Liu et al., 2021; Zhou et al., 2023). Briefly, stainless steel canisters and 2,4-  
129 dinitrophenylhydrazine (DNPH) cartridges were utilized to collect non-methane  
130 hydrocarbons (NMHCs) and oxygenated VOCs (OVOCs), respectively. NMHCs were  
131 quantified using a gas chromatograph (GC) coupled with a mass spectrometry detector  
132 (MSD), electron capture detector (ECD), and flame ionization detector (FID) (the GC-  
133 FID system for C<sub>2</sub>-C<sub>3</sub> species, and GC-MSD/ECD for other NMHCs). OVOC samples  
134 were analyzed by high-performance liquid chromatography. The accuracies for the  
135 NMHC measurements ranged from -22.58%–8.71%, with precisions of 0.86%–25.89%  
136 (Zhou et al., 2023). More details regarding the measurements can be found in  
137 Supplement S.1. ~~The collection devices, analytical instruments, quality controls, and~~  
138 ~~other measurement methods have been previously described (Lyu et al., 2019; Lyu et~~  
139 ~~al., 2020; Liu et al., 2021; Zhou et al., 2023).~~ From the ATMSYC dataset, we selected  
140 61 representative VOCs species and classified them into 20 categories, according to the  
141 SAPRC07 mechanism (Carter, 2010) to facilitate comparison with model predictions.

142 These species can be categorized into five groups: alkanes, alkenes, aromatics, alkynes,  
143 and formaldehydes (HCHO). Further details regarding these specific classifications are  
144 mentioned in Table S2.

145 Observations of O<sub>3</sub> and nitrogen dioxide (NO<sub>2</sub>) were collected from 28 ground  
146 sites, sourced from the Chinese Ministry of Ecology and Environment  
147 (<https://www.mee.gov.cn/>, last accessed on 20 April 2022), to assess the simulation  
148 performance of the modelled O<sub>3</sub> and NO<sub>2</sub>. To evaluate the impact of meteorological  
149 conditions, we also collected observation data of meteorological variables (temperature  
150 (T2), relative humidity (RH), wind speed (WS) and wind direction (WD)) from the  
151 nearest meteorological stations to the 28 sites from the Chinese Meteorological Agency  
152 (<http://data.cma.cn/en>, last accessed on 27 April 2022).

## 153 2.2. Model Configurations

154 The CMAQ version 5.2 model (Appel et al., 2018), coupled with the  
155 SAPRC07TIC mechanism and aerosol module AERO6i, was utilized to simulate air  
156 quality across China from June to August 2018 (Mao et al., 2022). Meteorological fields  
157 were generated using WRF version 4.2.1, employing a 1.0° × 1.0° resolution FNL  
158 reanalysis dataset from the National Centre for Atmospheric Research (NCAR). The  
159 specific settings of WRF were consistent with those described by Mao et al. (2022), and  
160 the simulation performance of the meteorological fields was verified (Mao et al., 2022).  
161 The modelling domain with a horizontal resolution of 36 km is shown in Figure 1,  
162 which divides China into seven regions: the North China Plain (NCP), Northwest,  
163 Northeast, Yangtze River Delta (YRD), Central China, Southwest, and South China  
164 (with a higher concentration of sites in the Pearl River Delta (PRD) region).

165 We utilized the Multi-resolution Emission Inventory for China (MEIC) v1.3 with  
166 a resolution of 0.25° × 0.25° in 2017 (<http://www.meicmodel.org>, last accessed on 25

167 January 2022) for anthropogenic emissions within China. For anthropogenic emissions  
168 outside of China, we employed the Regional Emission Inventory in Asia (REAS) v3.2  
169 in 2015 (<https://www.nies.go.jp/REAS/>, last accessed on 25 January 2022). Biogenic  
170 emissions were generated using the Model for Emissions of Gases and Aerosols from  
171 Nature (MEGAN) v2.1 (Guenther et al., 2012), which were then mapped to 27  
172 SAPRC07TIC species, including isoprene (ISOP),  $\alpha$ -pinene (APIN), and other BVOCs.  
173 Further details on the biogenic emissions can be found in (Li et al., 2022b). Open  
174 biomass burning emissions were processed using the Fire Inventory (NCAR FINN,  
175 <https://www2.acom.ucar.edu/modeling/finn-fire-inventory-ncar>, last accessed on 28  
176 January 2022).

177 Most emission inventories commonly employ a lumped mechanism to represent  
178 VOCs. Li et al. (2014) introduced a method to allocate individual non-methane VOC  
179 (NMVOC) emissions in the MEIC inventory to species groups using multiple chemical  
180 mechanisms, utilizing mechanism-specific mapping tables from Carter (2013). This  
181 method has been widely adopted in CTMs. In this study, we followed this approach and  
182 utilized a speciation profile processor called Spec DB, which is available from  
183 <https://intra.engr.ucr.edu/~carter/emitdb/>, provided by Carter, to generate the speciation  
184 profiles. The mapping scheme for the SAPRC07TIC mechanism in the MEIC and open  
185 biomass burning was updated based on the step-by-step assignment framework of the  
186 SAPRC07 mechanism provided by the MEIC team.

187 In this study, we examined the performance of CMAQ simulations during the  
188 observation period of the ATMSYC project. The days prior to 6 June were considered  
189 as a spin-up period. The simulated VOCs values at each site were matched with the  
190 observation time to obtain the average concentration during the same period. This  
191 duration was defined as the study period.



## 192 2.3. Adjustment of VOCs emissions

193 Emissions were adjusted for several species that exhibited significant deviations  
194 in simulations. The adjustment factors for emissions were determined by calculating  
195 the median of the ratio between observed and predicted values at 18 urban sites, which  
196 provided an average measure of the deviation for each species. Sensitivity experiments  
197 were conducted to examine the impact of the updated VOCs emissions on both  
198 predicted VOCs and O<sub>3</sub> levels. To quantify the effect of unit increments in VOCs on O<sub>3</sub>  
199 concentrations, the Relative Incremental Reactivity (RIR) was calculated. The RIR is a  
200 commonly used metric in observation-based model studies (Cardelino and Chameides,  
201 1995) to assess the sensitivity of O<sub>3</sub> to individual precursors such as NO<sub>x</sub> and various  
202 types of VOCs. The calculation of RIR is based on Equation (1):

$$203 \quad RIR(X) = \frac{(NO_3(X) - BO_3(X))/BO_3(X)}{(NX(X) - BX(X))/BX(X)} \quad (1)$$

204 In the equation, X represents a specific VOCs species, while B<sub>O<sub>3</sub></sub> and N<sub>O<sub>3</sub></sub> represent the  
205 O<sub>3</sub> concentrations in the base and adjusted emission case for X, respectively. The  
206 denominator on the right-hand side of the equation represents the relative change in  
207 emissions after the adjustment for X.

## 208 3. Results

### 209 3.1. Model performance evaluation

#### 210 3.1.1. Evaluation of O<sub>3</sub> and NO<sub>2</sub>

211 Figure 2 displays the performance of the CMAQ model for the maximum daily 8-  
212 hour average (MDA8) O<sub>3</sub> and NO<sub>2</sub> concentrations at 28 sites. Model performance was  
213 assessed using statistical parameters, including the normalized mean bias (NMB),  
214 normalized mean error (NME), and correlation coefficient (R). The specific values of  
215 these statistical metrics can be found in Table S3. The results indicated that the model  
216 predictions complied with the observations at most sites in the NCP, Central China, and

217 Southwest, with only slight underpredictions observed at Lanzhou's urban station (LZ-  
218 U; NMB = -0.18) and Shanghai's background station (SH-B; NMB = -0.16), and a  
219 slight overprediction at Shanghai's urban station (SH-U; NMB = 0.20). However, in the  
220 PRD, overpredictions of MDA8 O<sub>3</sub> were observed in locations such as Shenzhen's  
221 station (SZ; NMB = 0.39) and Foshan's station (FS; NMB = 0.32), despite the  
222 correlation coefficients being higher than the performance criteria at most sites. The  
223 CMAQ's NO<sub>2</sub> predictions exhibited underpredictions for most cities in the Northwest,  
224 PRD, and some background sites, but substantial overpredictions were evident in  
225 certain urban sites, such as Chengdu's urban station (CD-U; NMB = 0.92) and SZ  
226 (NMB = 0.52).

### 227 3.1.2. Evaluation of VOCs

228 Figure 3 presents the observed VOCs concentrations and corresponding CMAQ  
229 simulations across all the sites during the observation period. The proportions of the  
230 three categorized VOCs groups, namely alkanes, alkenes, and aromatics, are depicted  
231 in detail in Figure S1. The results revealed low predicted VOCs concentrations at most  
232 sites, with particularly markable underestimation in certain areas. Table S4 displays the  
233 mean values of O<sub>3</sub>, NO<sub>2</sub>, and total VOCs (TVOCs, encompassing the VOCs considered  
234 in this study) concentrations at the 28 sites throughout the study period. As indicated in  
235 Table 1, the predicted/observed ratio (referred to as ratio here after) of TVOCs is 0.74  
236 ± 0.40. The underprediction ranged from 2.05 to 50.61 ppbv (5.77% to 85.40%) at 24  
237 sites, while overpredictions occurred at four sites, namely SH-U, CU-U, Wuhan's  
238 background station (WH-B), and FS, with values ranging from 0.47 to 29.53 ppbv (1.92%  
239 to 89.96%). These findings suggested that the CMAQ model, employing the MEIC  
240 emission inventory, underpredicted TVOCs concentrations. Notably, the  
241 underprediction of TVOCs was more pronounced at sites located in the cities of

242 Lanzhou, Jinan, Shijiazhuang, Guiyang, and Zhengzhou, where TVOCs were  
243 underpredicted by factors of two to six.

244 The regional averages of the predicted and observed TVOCs were calculated by  
245 averaging the predictions and observations from all the sites in each region (Table S4).

246 The ~~observed~~ ratios of observed to predicted TVOCs ~~predictions~~ varied across regions  
247 as follows: YRD (1.04) > Southwest (0.92) > PRD (0.83) > Central China (0.71) > NCP  
248 (0.42) > Northwest (0.16). In Figure S2, despite having the highest observed TVOCs  
249 value (44.08 ppbv), the model results showed a lower concentration (7.04 ppbv) in the  
250 northwest region (specifically in Lanzhou), making it the region with the lowest  
251 predicted value. The predicted TVOCs concentration in the YRD region (Shanghai) was  
252 the closest to the observed value. However, Figure 3 shows that the VOCs  
253 concentrations were notably overpredicted at SH-U and underpredicted at SH-B. The  
254 southwest region appeared to have the best performance among all the regions, which  
255 could be due to the overpredicted TVOCs at CD-U, which offsets the underprediction  
256 at other sites. Overall, the predicted and observed TVOCs concentrations exhibited  
257 notable discrepancies in most regions and the performance varied across the regions.

258 Regarding the VOC components shown in Figure S2, alkanes consistently  
259 constituted as the most abundant group of VOCs in both observations (38.3% to 50.6%)  
260 and predictions (31.6% to 44.9%). This suggested that the predicted proportion of  
261 alkanes in TVOCs closely complied with the actual data. Alkenes typically ranked as  
262 the second highest VOC component in observations (14.9% to 31.2%), but they were  
263 underrepresented in the model (16.5% to 20.0%). The predicted proportions of  
264 aromatics (13.1% to 22.8%) and HCHO (15.3% to 28.9%) were higher than in the  
265 observations. In addition, alkynes were predicted to have a minor contribution to  
266 TVOCs. In the case of predicted aromatics and HCHO, their proportion in TVOCs often

267 ~~exceeded the observed results, which differed from the alkynes.~~ In terms of absolute  
268 concentrations, the underestimation of alkanes and alkenes was relatively pronounced,  
269 particularly in the NCP and Northwest regions. The model performed better in  
270 predicting the proportions of various VOCs species in the PRD and Southwest regions.

271 Figure 4 illustrates the ratios of O<sub>3</sub>, NO<sub>2</sub>, and various VOCs species at the 28 sites.  
272 The discrepancies in ratios between urban and background sites are presented in Figure  
273 S3. The ratio of alkanes is  $0.53 \pm 0.38$  (median  $\pm$  standard deviation), indicating an  
274 underprediction of  $5.65 \pm 6.81$  ppbv from a concentration standpoint (Table 1). Notably,  
275 the alkanes whose reaction rate constant with hydroxyl radical (OH) between  $5 \times 10^2$   
276 and  $2.5 \times 10^3$  ppm<sup>-1</sup> min<sup>-1</sup> (ALK2) exhibited the most notable underprediction. The  
277 predictions for aromatics showed minor deviations across different sites, but the median  
278 ratio was close to one, except for ARO2MN, which was substantially underpredicted  
279 with a ratio of  $0.31 \pm 0.38$  ( $0.32 \pm 0.46$  at urban sites), and benzene (BENZ), which was  
280  $2.75 \pm 1.97$  at urban sites (Table S5). ~~Regarding alkenes, t~~The ratios for the seven  
281 alkenes were generally high ( $0.51 \pm 0.48$  for alkenes), indicating underprediction in  
282 most sites. Particularly, 1,3-butadiene (BDE13) exhibited a notable low ratio, possibly  
283 due to its reallocation from the underpredicted alkenes whose reaction rate constant is  
284 greater than  $7 \times 10^4$  ppm<sup>-1</sup> min<sup>-1</sup> with OH (OLE2) and the allocation factor may not be  
285 universally applicable across regions. Furthermore, the predicted ~~concentration content~~  
286 of acetylene (ACYE) was lower ~~than observation~~ at all sites ( $0.41 \pm 0.47$  for alkynes),  
287 while the ~~predicted~~ HCHO was slightly overpredicted ( $1.21 \pm 1.61$  for HCHO).  
288 Considering that the observed VOCs species primarily originated from anthropogenic  
289 emissions and ~~that~~ the majority of emitted VOCs were contributed by the MEIC, the  
290 ratios between urban and background sites could verify whether the MEIC emission  
291 inventory adequately reflected the differences between urban and background areas.

## 292 3.2. Adjusting VOCs emissions and their impacts on O<sub>3</sub> predictions

293 These findings indicated a bias between the model-predicted VOCs and observed  
294 ambient VOCs concentrations. To evaluate the impact of these biases on O<sub>3</sub> predictions,  
295 we modified the VOCs emissions of the MEIC based on the differences between  
296 observations and predictions. Previous studies have adjusted emission inventories to  
297 match observed constraints for predicting VOCs and O<sub>3</sub> in specific cities (Wu et al.,  
298 2022; Wang et al., 2020). Considering the temporal and spatial variability of the 28 sites,  
299 we calculated the median ratio of VOCs for the 18 urban sites. We selected coefficients  
300 for six representative AVOCs species with deviations exceeding 2.0 times the median,  
301 including ALK2, ARO2MN, BENZ, the alkenes (excluding ethene) whose reaction rate  
302 constant is less than  $7 \times 10^4 \text{ ppm}^{-1} \text{ min}^{-1}$  with OH (OLE1), propene (PRPE), and ACYE,  
303 and adjusted their emission rates in the MEIC, resulting in six new cases. Additionally,  
304 we conducted a case (case\_all) that incorporated the aforementioned adjustments and a  
305 case in which NO<sub>x</sub> was adjusted by 1.5 based on observational constraints. The  
306 adjustment factors for the eight new cases are provided in Table 2.

307 The impact of adjusting VOCs emissions on the concentrations of O<sub>3</sub> and VOCs is  
308 presented in Table S6. The underprediction of simulated VOCs and NO<sub>2</sub> values was  
309 largely reduced for the new case, as indicated in the six cases with single-species  
310 changes and the case\_all. In Table S7, the ratio of TVOCs in case\_all was modified to  
311  $0.86 \pm 0.47$ , demonstrating improved performance in VOCs compared to the base case.  
312 However, it was worth noting that even after the emission adjustment, the predicted  
313 VOCs concentrations remained lower than the observations (particularly for  
314 case\_BENZ). This discrepancy resulted from the varying reactivities of different VOC  
315 species and NO<sub>x</sub> in atmospheric chemical reactions, leading to different levels of  
316 depletion. Additionally, both measured and modelled concentrations were subject to

317 photochemical losses (Ma et al., 2022b; Shao et al., 2011). The increased VOCs  
318 concentrations resulted in higher O<sub>3</sub> concentrations. Based on the data presented in  
319 Tables S6 and S8, the constrained species ALK2, ARO2MN, OLE1, and PRPE, guided  
320 by observational data, contributed to an increase in O<sub>3</sub> concentration, especially in  
321 case\_all, which led to a more pronounced overpredictions ranging from 0.62% to 6.27%  
322 across all the sites. In contrast, increasing NO<sub>x</sub> had a positive effect and reduced the O<sub>3</sub>  
323 concentration.

324 To illustrate regional pollution levels on a broader scale, Figure 5 displays the  
325 average concentrations of O<sub>3</sub>, NO<sub>2</sub>, and the six previously mentioned VOCs species  
326 studied in China during the specified period.

327 High O<sub>3</sub> levels were particularly prominent in most areas of the NCP, the eastern  
328 part of the Northwest, and the Sichuan Basin in the Southwest. NO<sub>2</sub> concentrations  
329 were elevated in the NCP, YRD, and PRD regions, as well as in certain megacities. The  
330 spatial distribution of various VOCs, derived from TVOCs emissions in the MEIC,  
331 exhibited broad consistency, with higher concentrations observed in south-eastern  
332 China. Megacities, akin to NO<sub>2</sub>, displayed elevated VOCs levels. Different cities  
333 exhibited VOCs originating from various sources. ALK2 demonstrated high  
334 concentrations in individual cities but less than 1 ppbv in other regions; thus, displaying  
335 stronger geographical characteristics compared to the other five VOCs. ARO2MN  
336 exhibited the lowest average concentration but exerted a substantial influence on O<sub>3</sub>  
337 due to its higher reactivity. Figure S4 illustrates the effects of altering the emission rates  
338 of NO<sub>x</sub> and VOCs in seven scenarios across China. The left panel displays the  
339 concentrations in the new cases, while the middle and right panels show the  
340 ~~concentration~~ differences for corresponding species and O<sub>3</sub> between the new cases and  
341 the base case, respectively. Spatial variations in NO<sub>2</sub> and VOCs exhibited similarities.

342 The increase in NO<sub>2</sub> was more pronounced in the NCP and YRD regions, where NO<sub>2</sub>  
343 concentrations was consistently high. Previous studies indicate that the NCP and YRD  
344 regions are predominantly limited by VOCs during the summer (Li et al., 2017b; Lyu  
345 et al., 2019; Liu et al., 2021), resulting in either no change or a reduction in O<sub>3</sub> when  
346 NO<sub>2</sub> increases. Conversely, in other areas with low NO<sub>2</sub> concentrations, O<sub>3</sub>  
347 concentrations increased by 0 to 10 ppbv. BENZ was the only compound whose  
348 concentration decreased, and its impact on O<sub>3</sub> in different regions mirrored that of NO<sub>2</sub>,  
349 albeit at a much lower concentration. The increased emissions of ALK2, ARO2MN,  
350 ACYE, OLE1, and PRPE favoured O<sub>3</sub> production, with the most notable effects  
351 observed in the NCP, YRD, and other metropolitan areas. Among these compounds,  
352 OLE1 exhibited the strongest effect, while ACYE had a minimal influence.

353 The section 2.3 describes the calculation of the RIR values, which were used to  
354 demonstrate the sensitivity of the model-simulated O<sub>3</sub> to VOCs constrained by  
355 observations in different locations. Figure S5 presents the variations in RIR values for  
356 the six VOCs across the 28 sites. OLE1, PRPE, and ARO2MN exhibited a higher RIR  
357 values. Urban areas within the same city displayed a higher RIR values compared to  
358 the background areas. With the exception of Chengdu, Guiyang, Lanzhou's background  
359 station (LZ-B), Guangzhou's background station (GZ-B), and Zhaoqing's station (ZQ),  
360 where O<sub>3</sub> generation was more sensitive to PRPE, other areas showed a greater impact  
361 of OLE1 concentration on O<sub>3</sub>, indicating that adjusting the emission rate of alkenes in  
362 the emission inventory was crucial for simulating changes in O<sub>3</sub> concentrations. For  
363 instance, improvements could be made in LZ-U, Huizhou's station (HZ), and  
364 Jiangmen's station (JM), where O<sub>3</sub> concentrations were underpredicted in the base case.  
365 Special attention should be given to the sites with high RIR values such as SH-U, CD-  
366 U, SZ, Zhuhai's station (ZH), and others, as O<sub>3</sub> generation in these locations will be

367 highly sensitive to changes in the local VOCs emission inventory. Moreover, ALK2,  
368 ACYE, and BENZ had minimal effects on O<sub>3</sub>, and BENZ even exhibited a negative  
369 RIR values at certain sites.

370 These findings indicated a notable improvement in the underprediction of VOCs  
371 when adjustments were made based on VOCs observations. However, the elevated  
372 VOCs concentrations in the model could lead to increased O<sub>3</sub> formation, thereby  
373 enhancing the model's accuracy in areas where both VOCs and O<sub>3</sub> were underpredicted.  
374 Nonetheless, this adjustment will unavoidably worsen any existing overprediction of  
375 O<sub>3</sub> in the model.

## 376 4. Discussions

### 377 4.1. Large bias in TVOCs predictions at specific sites

378 Significant discrepancies between predicted and observed TVOCs were observed  
379 in Lanzhou, Jinan, Shijiazhuang, and Zhengzhou. Lanzhou and Shijiazhuang have  
380 developed petrochemical industries, where high concentrations of VOCs are frequently  
381 detected downwind of industrial areas (Guan et al., 2020; Guo et al., 2022). Figure 3  
382 illustrates that alkanes, alkenes, and aromatic<sub>s</sub> were substantially underpredicted due to  
383 inadequate prediction of industrial areas with high VOCs emissions in the MEIC. Jinan  
384 and Zhengzhou experienced severe air pollution due to heavy industry and traffic  
385 (Zhang et al., 2017; Wang et al., 2022c). The simulated levels of TVOCs were  
386 substantially lower than the observed levels, with alkenes exhibiting an even greater  
387 inaccuracy, being more than 10 times lower in Jinan. At certain sites, the simulated  
388 TVOCs exceeded the measurements, including the CD-U, SH-U, WH-B, and FS sites.  
389 In CD-U, the predicted TVOCs were almost double the measured values, whereas they  
390 were underpredicted in CD-B. In Chengdu, VOCs emissions were dominated by  
391 LPG/NG usage and vehicle emissions in summer, with a higher proportion of low-



392 carbon alkanes compared to other cities in China (Xiong et al., 2021). It is most likely  
393 that VOC emissions in CD-U were overpredicted. This could also cause high biases of  
394 HCHO, which is mostly generated from secondary production in VOC photochemical  
395 reactions (Atkinson and Arey, 2003; Wu et al., 2023). ~~Clearly, the MEIC overpredicted~~  
396 ~~VOCs emissions in CD-U, particularly for HCHO (Atkinson and Arey, 2003; Wu et al.,~~  
397 ~~2023).~~ In SH-U, characterized by a dense population, the simulation of alkenes,  
398 aromatics, and HCHO was approximately twice that of the measurements. This aligns  
399 complied with the report by Wang et al. (2020) stating that observation-constrained  
400 aromatic emissions were roughly half of the estimates provided by the MEIC in  
401 Shanghai, 2015. Peng et al. (2023) also observed inconsistencies between the trend of  
402 non-methane hydrocarbon emissions in Shanghai from 2009 to 2015 and the growth  
403 trend indicated by the MEIC (Li et al., 2019), suggesting the effectiveness of local  
404 pollution control measures. However, SH-B was situated in the easternmost part of  
405 Chongming Island, which had the minimal local emissions at the 36 km grid resolution.  
406 This likely explains the differences observed between the urban background areas in  
407 Shanghai. In the cases of WH-B and FS, which demonstrated excellent model  
408 performance for VOCs, only the overprediction of aromatics was more pronounced.

409 Heavy O<sub>3</sub> pollution events, primarily limited by VOCs, have been frequently  
410 observed in the PRD region since its rapid development in the last century (Chan et al.,  
411 2006; Shao et al., 2009; Li et al., 2014). In the PRD region, slightly lower TVOCs  
412 simulations were observed at most sites, primarily due to the underestimation of alkanes  
413 and alkenes, while aromatics and HCHO were overestimated. Furthermore, the  
414 differences in VOCs components among the cities in the PRD region could be attributed  
415 to local industry characteristics, and variations in prevention and control policies. For  
416 instance, although the TVOC concentration was well modelled in FS, the simulated

417 ethene (ETHE) accounted for 35% of the alkenes, lower than the observed fraction of  
418 over 50%. In addition, the predicted HCHO (3.66 ppbv) was much higher than the  
419 observed value (0.42 ppbv).~~For instance, observed ethene (ETHE) in FS accounted for~~  
420 ~~over 50% of the alkenes, whereas simulations accounted for only 35%.~~ The predicted  
421 ETHE ~~ratio~~ in ZH was higher (50% of alkenes) than the ~~observationed ratio~~ (20% of  
422 alkenes), while other cities exhibited similar ETHE percentages. Moreover, the  
423 proportion of ISOP in Guangzhou's alkenes was higher than that in other PRD cities,  
424 suggesting effective control of local anthropogenic alkene emissions, consistent with  
425 the findings of Zhao et al. (2022).

#### 426 4.2. Urban-background evaluation

427 Differences in atmospheric VOCs among urban and background areas have been  
428 extensively demonstrated (Sillman, 1999; Shao et al., 2020). As depicted in Figure 6,  
429 we compared the average performance of the model for 18 urban sites and 10  
430 background sites. In urban areas, the predicted TVOCs concentration (23.76 ppbv) was  
431 lower than the observed concentration (32.46 ppbv), primarily due to the  
432 underprediction of alkanes, alkenes, and alkynes. Predicted aromatics and HCHO  
433 exhibited higher proportions and concentrations compared to the observations. In the  
434 background areas, TVOCs were also underpredicted, with concentrations lower than  
435 those in urban areas, as indicated by both the observed and predicted values. Each of  
436 the five VOCs showed lower predictions, with alkanes exhibiting the most notable  
437 disparity, with a negative bias of 6.91 ppbv compared to the observation values~~with a~~  
438 ~~decrease of 6.91 ppbv compared to the observed values~~. This suggested that the model  
439 underpredicted alkanes in urban areas, which were predominantly derived from the  
440 petrochemical industry or fuel evaporation (Wang et al., 2022a). The predicted  
441 proportions of alkanes, aromatics, and HCHO exhibited urban-background differences

442 consistent with the observations, reflecting the characteristics of urban and background  
443 areas in the model. These differences were well represented in our horizontal grid  
444 resolution of only 36 km. Overall, the CMAQ model captured the characteristics of  
445 urban and background areas in different regions~~different regions and urban background~~  
446 ~~areas~~ but underestimated the concentrations of certain individual VOC species.

447 The ratios distinguished between urban and background areas are presented in  
448 Figure S3. The comparison revealed that the alkanes were more prominently  
449 underpredicted in the background area than in the urban area. Xylene (XYL), 1,2,4-  
450 trimethylbenzene (B124), OLE1, OLE2, and PRPE were also underpredicted to a  
451 greater extent in the background area. This could be attributed to the scarcity of  
452 background sites or the model's underprediction of VOCs emissions in the background  
453 area. The model's performance in simulating ISOP, a BVOC, in urban areas was not as  
454 satisfactory as in the background areas, which was consistent with the findings of Ma  
455 et al. (2021) suggesting that MEGAN could underestimate the emissions from urban  
456 green spaces. APIN, an important a notable~~monoterpene, originating from~~~~including~~  
457 anthropogenic emissions from biomass burning and VCPs, could be either  
458 underpredicted or disregarded (Wang et al., 2022b; McDonald et al., 2018), resulting in  
459 common underprediction with a median ratio of five in urban-background areas.  
460 Additionally, the simulated HCHO concentrations were higher in the urban areas.  
461 Overall, these results indicated that the model generally performed better for  
462 anthropogenic VOCs in the urban areas. However, there were still a few notable outliers  
463 and significant deviations for a majority of VOCs, particularly those with high chemical  
464 reactivity. These deviations will inevitably impact the model's calculation of  
465 photochemical reactions involved in O<sub>3</sub> generation.

466 4.3. Implications and suggestions

467 Accurately predicting VOCs is crucial for O<sub>3</sub> modelling. However, due to limited  
468 measurement data and uncertainties in emission inventories, accurately simulating the  
469 VOCs across China using CTMs remains challenging.

470 Considerable efforts have been dedicated to the development of VOCs emission  
471 inventories in recent years (Li et al., 2019; An et al., 2021; Chang et al., 2022). However,  
472 our findings indicate a substantial variation in the model performance of VOCs across  
473 different regions and species. Therefore, the inclusion of accurate local emission factors,  
474 activity data, and source profiles is essential. Sha et al. (2021) compiled an integrated  
475 dataset of AVOCs source profiles in China, emphasizing the need for supplementary  
476 and timely updates to these profiles in the future. Apart from anthropogenic emissions,  
477 model resolution, ~~and~~ chemical mechanisms, meteorological conditions, and BVOCs  
478 emissions also contribute to the uncertainty of VOCs modelling, thereby affecting the  
479 performance of O<sub>3</sub> modelling (Zhang et al., 2021; Wang et al., 2021; Liu et al., 2022).

480 High-resolution models require higher emission inventory resolution (Li et al.,  
481 2022; An et al., 2021), which can improve simulation performance to a certain extent.  
482 Given the large scope of the model used in this study and the 0.25° × 0.25° horizontal  
483 resolution of the MEIC inventory, a resolution of 36 km was chosen to balance  
484 computational efficiency and the preservation of information from the emission  
485 inventory, but inevitably results in deviation of the modelled VOCs and other elements.  
486 On the one hand, urban and background sites in close proximity may be assigned to the  
487 same grid in the model, as shown in Table S3, making it difficult to distinguish the  
488 differences in modelled VOCs between urban and background sites in cities such as  
489 Shijiazhuang, Jinan, Wuhan, and Guiyang; on the other hand, in real atmospheres, even  
490 with close proximity, the observed VOCs may differ greatly in concentration, which is  
491 challenging to capture in a coarse-resolution model. When applying coarse-resolution

492 emission inventories, increasing the model resolution can enhance the spatial  
493 correlation between observed and predicted concentrations, but does not always  
494 improve simulation performance (Zheng et al., 2021). High-resolution models may  
495 introduce more emission mapping errors, which can be reduced by using coarse-  
496 resolution model grids (Zheng et al., 2021). Therefore, addressing this issue requires  
497 not only finer model resolution but also improved emission inventories.

498 The SAPRC07~~the~~TIC chemical mechanism used in this study has been proven  
499 reliable in previous model applications (Qin et al., 2022), reducing the computational  
500 effort compared to the explicit MCM mechanism (Li et al., 2015) while retaining the  
501 chemical reactivity of various VOCs. However, the lumped VOCs species contain more  
502 VOCs species than those in corresponding observations. Therefore, if both the emission  
503 inventory and model are sufficiently accurate, the predicted values should theoretically  
504 be higher.

505 Notably, this study revealed that the model overpredicted HCHO, while some  
506 previous studies tend to show underprediction (Luecken et al., 2018; Li et al., 2022b).  
507 The biases could result from uncertainties in VOC emissions, chemical mechanisms,  
508 model resolution, etc. In general, HCHO is mainly contributed by oxidations of reactive  
509 VOCs such as ISOP, ETHE, PRPE, and toluene (TOLU) (Simpson et al., 2010; Wei et  
510 al., 2023; Wu et al., 2023). The overprediction of HCHO suggests that there may be  
511 excessive emissions of these VOCs or that the reaction rates of some VOCs with OH  
512 radicals were overpredicted in the model. Secondly, HCHO predictions could vary by  
513 25–40% with different chemical mechanisms, likely due to differences in hydrogen  
514 oxide radicals (HO<sub>x</sub>) and VOCs grouping (Knote et al., 2015; Luecken et al., 2018).  
515 Lastly, finer model resolution could improve the representation of HCHO, especially at  
516 grids where HCHO was substantially affected by point sources (e.g., petrochemical

517 facilities), as has been reported in (Parrish et al., 2012). Considering HCHO is an  
518 important source of HO<sub>x</sub> radicals and drives ozone production (Wittrock et al., 2006;  
519 Li et al., 2021a), more investigations are warranted to improve the model performance  
520 of HCHO in the future.

521 Meteorology bias also contributed to some bias of the VOCs predictions. We added  
522 evaluation of the meteorology predictions in this study, and the results are shown in  
523 Table S9 and S10. The results are consistent with other studies in China (Mao et al.,  
524 2022; Wang et al., 2021). It is observed that temperature is overpredicted at most sites,  
525 while RH is mostly underpredicted. The combination of high temperature and low RH  
526 facilitates the consumption of VOCs through photochemical reactions, which may  
527 explain the tendency of our modelled VOCs to be underestimated. But we believe it is  
528 insufficient to account for the underestimation of low-reactivity VOC species (mainly  
529 alkanes). Furthermore, the modelled wind speeds slightly exceed the observations,  
530 which may also contribute to VOCs underprediction (Table S10). While the bias in  
531 meteorological conditions contributes to the underestimation of modelled VOCs, the  
532 underestimated VOCs emissions is the key factor for the VOCs underprediction across  
533 most of the cities.

534 In this study, the adjustment of VOCs emissions resulted in increased predicted  
535 emission levels, subsequently leading to higher O<sub>3</sub> predictions. However, these  
536 adjustments are simplistic and fail to account for regional variations in VOCs biases.  
537 The accuracy of VOCs measurement data is also crucial. Therefore, there is a need to  
538 promote the establishment of a national O<sub>3</sub> precursor monitoring network and develop  
539 a standardized framework with quality control systems. This would facilitate the  
540 comparability of VOCs measurements between regions, thereby supporting related  
541 research and the implementation of collaborative regional prevention and control

542 measures.

## 543 **5. Conclusion**

544 In this study, we conducted a comprehensive evaluation of the simulation  
545 performance of VOCs using the CMAQ model and investigated the influence of  
546 predicted VOCs on O<sub>3</sub> formation. The inclusion of summertime-observed VOCs data  
547 from the ATMSYC project for 28 sites in China enhanced the spatiotemporal  
548 comparability of our model evaluation.

549 During the study period, TVOCs were found to be underpredicted by  $14.1 \pm 13.2$   
550 ppbv at 24 sites, except for SH-U, CD-U, WH-B, and FS. Despite some sites exhibiting  
551 similar TVOCs concentrations, differences still persisted in their specific components.  
552 ~~After Through~~ considering the uncertainties of the MEIC ~~inventory model~~ and relevant  
553 factors, we found several sites with substantial inaccuracies, such as Jinan,  
554 Shijiazhuang, Lanzhou, Chengdu, and Guiyang. The model's performance in predicting  
555 TVOCs and their components varied across regions, with better predictions observed  
556 in urban areas compared to background areas.

557 Alkanes, alkenes, ARO2MN, and alkynes are generally underpredicted, with ratios  
558 of  $0.53 \pm 0.38$ ,  $0.51 \pm 0.48$ ,  $0.31 \pm 0.38$ , and  $0.41 \pm 0.47$ , respectively, ~~except for HCHO~~  
559 ~~which is overpredicted, with the ratio of  $1.21 \pm 1.61$~~ . In urban areas, the CMAQ model  
560 exhibited underpredictions for OLE1, ALK2, ARO2MN, PRPE, ACYE, and NO<sub>x</sub>,  
561 ranging from 2.0 to 4.6 times, while overpredicting BENZ by 2.75 times. For sensitivity  
562 experiments, their emissions were adjusted and their impact on O<sub>3</sub> and VOCs was  
563 evaluated. These adjustments improved the model's VOCs performance, resulting in a  
564 change in the ratio of total VOCs to  $0.86 \pm 0.47$ . However, the increased VOCs  
565 contributed to higher reactivity, exacerbating O<sub>3</sub> overpredictions by 0.62% to 6.27%  
566 across the sites. Consequently, RIR values were calculated to depict the varying

567 reactivities of VOCs in different regions, with OLE1, PRPE, and ARO2MN  
568 contributing the highest RIR values during the study period.

569 Due to the uncertainties ~~inaccuracies~~ present in current VOCs emission inventories,  
570 notable efforts are needed to enhance the development and updating of emission  
571 inventories, particularly in regions characterized by developed industries, evolving  
572 energy structures, and relatively underdeveloped conditions. It is only through  
573 improving the accuracy of VOCs emission inventories that we can ensure reliable  
574 model performance in predicting O<sub>3</sub> levels, thereby establishing a solid foundation for  
575 addressing the escalating issue of O<sub>3</sub> pollution.

576

#### 577 **Acknowledgements**

578 This work was supported by the National Natural Science Foundation of China  
579 (42007187, 42021004, ~~42277095~~).

580



581 **References**

- 582 An, J., Huang, Y., Huang, C., Wang, X., Yan, R., Wang, Q., Wang, H., Jing, S., Zhang, Y., Liu, Y., Chen,  
583 Y., Xu, C., Qiao, L., Zhou, M., Zhu, S., Hu, Q., Lu, J., and Chen, C.: Emission inventory of air pollutants  
584 and chemical speciation for specific anthropogenic sources based on local measurements in the  
585 Yangtze River Delta region, China, *Atmos. Chem. Phys.*, 21, 2003-2025, 10.5194/acp-21-2003-  
586 2021, 2021.
- 587 Appel, W., Napelenok, S., Hogrefe, C., Pouliot, G., Foley, K. M., Roselle, S. J., Pleim, J. E., Bash, J.,  
588 Pye, H. O. T., Heath, N., Murphy, B., and Mathur, R.: Overview and Evaluation of the Community  
589 Multiscale Air Quality (CMAQ) Modeling System Version 5.2, *Air Pollution Modeling and its*  
590 *Application XXV*, Cham, 69-73,
- 591 Atkinson, R. and Arey, J.: Atmospheric Degradation of Volatile Organic Compounds, *Chemical*  
592 *Reviews*, 103, 4605-4638, 10.1021/cr0206420, 2003.
- 593 Cardelino, C. A. and Chameides, W. L.: An observation-based model for analyzing ozone precursor  
594 relationships in the urban atmosphere, *J Air Waste Manag Assoc*, 45, 161-180,  
595 10.1080/10473289.1995.10467356, 1995.
- 596 Carter, W. P. L.: Development of the SAPRC-07 chemical mechanism, *Atmospheric Environment*,  
597 44, 5324-5335, 10.1016/j.atmosenv.2010.01.026, 2010.
- 598 Carter, W. P. L.: Development of an improved chemical speciation database for processing  
599 emissions of volatile organic compounds for air quality models, report available at:  
600 <https://intra.engr.ucr.edu/~carter/emitdb/>, 2013.
- 601 Chan, L., Chu, K., Zou, S., Chan, C., Wang, X., Barletta, B., Blake, D., Guo, H., and Tsai, W.:  
602 Characteristics of nonmethane hydrocarbons (NMHCs) in industrial, industrial-urban, and  
603 industrial-suburban atmospheres of the Pearl River Delta (PRD) region of south China, *Journal of*  
604 *Geophysical Research*, 111, 10.1029/2005jd006481, 2006.
- 605 Chang, X., Zhao, B., Zheng, H., Wang, S., Cai, S., Guo, F., Gui, P., Huang, G., Wu, D., Han, L., Xing,  
606 J., Man, H., Hu, R., Liang, C., Xu, Q., Qiu, X., Ding, D., Liu, K., Han, R., Robinson, A. L., and Donahue,  
607 N. M.: Full-volatility emission framework corrects missing and underestimated secondary organic  
608 aerosol sources, *One Earth*, 5, 403-412, 10.1016/j.oneear.2022.03.015, 2022.
- 609 Dang, R., Liao, H., and Fu, Y.: Quantifying the anthropogenic and meteorological influences on  
610 summertime surface ozone in China over 2012-2017, *Sci Total Environ*, 754, 142394,  
611 10.1016/j.scitotenv.2020.142394, 2021.
- 612 Emery, C., Liu, Z., Russell, A. G., Odman, M. T., Yarwood, G., and Kumar, N.: Recommendations on  
613 statistics and benchmarks to assess photochemical model performance, *J Air Waste Manag Assoc*,  
614 67, 582-598, 10.1080/10962247.2016.1265027, 2017.
- 615 Gong, K., Li, L., Li, J., Qin, M., Wang, X., Ying, Q., Liao, H., Guo, S., Hu, M., Zhang, Y., and Hu, J.:  
616 Quantifying the impacts of inter-city transport on air quality in the Yangtze River Delta urban  
617 agglomeration, China: Implications for regional cooperative controls of PM<sub>2.5</sub> and O<sub>3</sub>, *Sci Total*  
618 *Environ*, 779, 146619, 10.1016/j.scitotenv.2021.146619, 2021.
- 619 Guan, Y., Wang, L., Wang, S., Zhang, Y., Xiao, J., Wang, X., Duan, E., and Hou, L.: Temporal variations  
620 and source apportionment of volatile organic compounds at an urban site in Shijiazhuang, China,  
621 *J Environ Sci (China)*, 97, 25-34, 10.1016/j.jes.2020.04.022, 2020.
- 622 Guenther, A., Karl, T., Harley, P., Wiedinmyer, C., Palmer, P. I., and Geron, C.: Estimates of global  
623 terrestrial isoprene emissions using MEGAN (Model of Emissions of Gases and Aerosols from  
624 Nature), *Atmos. Chem. Phys.*, 6, 3181-3210, 10.5194/acp-6-3181-2006, 2006.
- 625 Guenther, A., Jiang, X., Heald, C., Sakulyanontvittaya, T., Duhl, T., Emmons, L., and Wang, X.: The  
626 Model of Emissions of Gases and Aerosols from Nature version 2.1 (MEGAN2.1): an extended and  
627 updated framework for modeling biogenic emissions, *Geoscientific Model Development*, 5, 1471-  
628 1492, 10.5194/gmd-5-1471-2012, 2012.
- 629 Guo, W., Yang, Y., Chen, Q., Zhu, Y., Zhang, Y., Zhang, Y., Liu, Y., Li, G., Sun, W., and She, J.: Chemical  
630 reactivity of volatile organic compounds and their effects on ozone formation in a petrochemical

631 industrial area of Lanzhou, Western China, *Sci Total Environ*, 839, 155901,  
632 10.1016/j.scitotenv.2022.155901, 2022.

633 Hu, J., Chen, J., Ying, Q., and Zhang, H.: One-year simulation of ozone and particulate matter in  
634 China using WRF/CMAQ modeling system, *Atmospheric Chemistry and Physics*, 16, 10333-10350,  
635 10.5194/acp-16-10333-2016, 2016.

636 Hu, J., Wang, P., Ying, Q., Zhang, H., Chen, J., Ge, X., Li, X., Jiang, J., Wang, S., Zhang, J., Zhao, Y.,  
637 and Zhang, Y.: Modeling biogenic and anthropogenic secondary organic aerosol in China,  
638 *Atmospheric Chemistry and Physics*, 17, 77-92, 10.5194/acp-17-77-2017, 2017.

639 Kelly, J. M., Doherty, R. M., O'Connor, F. M., and Mann, G. W.: The impact of biogenic,  
640 anthropogenic, and biomass burning volatile organic compound emissions on regional and  
641 seasonal variations in secondary organic aerosol, *Atmospheric Chemistry and Physics*, 18, 7393-  
642 7422, 10.5194/acp-18-7393-2018, 2018.

643 Knote, C., Tuccella, P., Curci, G., Emmons, L., Orlando, J. J., Madronich, S., Baró, R., Jiménez-  
644 Guerrero, P., Luecken, D., Hogrefe, C., Forkel, R., Werhahn, J., Hirtl, M., Pérez, J. L., San José, R.,  
645 Giordano, L., Brunner, D., Yahya, K., and Zhang, Y.: Influence of the choice of gas-phase mechanism  
646 on predictions of key gaseous pollutants during the AQMEII phase-2 intercomparison,  
647 *Atmospheric Environment*, 115, 553-568, 10.1016/j.atmosenv.2014.11.066, 2015.

648 Kroll, J. H. and Seinfeld, J. H.: Chemistry of secondary organic aerosol: Formation and evolution of  
649 low-volatility organics in the atmosphere, *Atmospheric Environment*, 42, 3593-3624,  
650 10.1016/j.atmosenv.2008.01.003, 2008.

651 Kurokawa, J. and Ohara, T.: Long-term historical trends in air pollutant emissions in Asia: Regional  
652 Emission inventory in ASia (REAS) version 3, *Atmos. Chem. Phys.*, 20, 12761-12793, 10.5194/acp-  
653 20-12761-2020, 2020.

654 Li, C., Liu, Y., Cheng, B., Zhang, Y., Liu, X., Qu, Y., An, J., Kong, L., Zhang, Y., Zhang, C., Tan, Q., and  
655 Feng, M.: A comprehensive investigation on volatile organic compounds (VOCs) in 2018 in Beijing,  
656 China: Characteristics, sources and behaviours in response to O<sub>3</sub> formation, *Sci Total Environ*, 806,  
657 150247, 10.1016/j.scitotenv.2021.150247, 2022a.

658 Li, J., Cleveland, M., Ziemba, L. D., Griffin, R. J., Barsanti, K. C., Pankow, J. F., and Ying, Q.: Modeling  
659 regional secondary organic aerosol using the Master Chemical Mechanism, *Atmospheric  
660 Environment*, 102, 52-61, 10.1016/j.atmosenv.2014.11.054, 2015.

661 Li, J., Lu, K., Lv, W., Li, J., Zhong, L., Ou, Y., Chen, D., Huang, X., and Zhang, Y.: Fast increasing of  
662 surface ozone concentrations in Pearl River Delta characterized by a regional air quality monitoring  
663 network during 2006–2011, *Journal of Environmental Sciences*, 26, 23-36, 10.1016/s1001-  
664 0742(13)60377-0, 2014.

665 Li, J., Xie, X., Li, L., Wang, X., Wang, H., Jing, S., Ying, Q., Qin, M., and Hu, J.: Fate of Oxygenated  
666 Volatile Organic Compounds in the Yangtze River Delta Region: Source Contributions and Impacts  
667 on the Atmospheric Oxidation Capacity, *Environ Sci Technol*, 56, 11212-11224,  
668 10.1021/acs.est.2c00038, 2022b.

669 Li, K., Jacob, D. J., Shen, L., Lu, X., De Smedt, I., and Liao, H.: Increases in surface ozone pollution in  
670 China from 2013 to 2019: anthropogenic and meteorological influences, *Atmospheric Chemistry  
671 and Physics*, 20, 11423-11433, 10.5194/acp-20-11423-2020, 2020.

672 Li, K., Chen, L., Ying, F., White, S. J., Jang, C., Wu, X., Gao, X., Hong, S., Shen, J., Azzi, M., and Cen,  
673 K.: Meteorological and chemical impacts on ozone formation: A case study in Hangzhou, China,  
674 *Atmospheric Research*, 196, 40-52, 10.1016/j.atmosres.2017.06.003, 2017b.

675 Li, K., Jacob, D. J., Liao, H., Qiu, Y., Shen, L., Zhai, S., Bates, K. H., Sulprizio, M. P., Song, S., Lu, X.,  
676 Zhang, Q., Zheng, B., Zhang, Y., Zhang, J., Lee, H. C., and Kuk, S. K.: Ozone pollution in the North  
677 China Plain spreading into the late-winter haze season, *Proceedings of the National Academy of  
678 Sciences*, 118, 10.1073/pnas.2015797118, 2021a.

679 Li, L., Xie, F., Li, J., Gong, K., Xie, X., Qin, Y., Qin, M., and Hu, J.: Diagnostic analysis of regional ozone  
680 pollution in Yangtze River Delta, China: A case study in summer 2020, *Sci Total Environ*, 812,  
681 151511, 10.1016/j.scitotenv.2021.151511, 2022.

682 Li, L., Hu, J., Li, J., Gong, K., Wang, X., Ying, Q., Qin, M., Liao, H., Guo, S., Hu, M., and Zhang, Y.:  
683 Modelling air quality during the EXPLORE-YRD campaign – Part II. Regional source apportionment  
684 of ozone and PM<sub>2.5</sub>, *Atmospheric Environment*, 247, 10.1016/j.atmosenv.2020.118063, 2021b.

685 Li, M., Liu, H., Geng, G., Hong, C., Liu, F., Song, Y., Tong, D., Zheng, B., Cui, H., Man, H., Zhang, Q.,  
686 and He, K.: Anthropogenic emission inventories in China: a review, *National Science Review*, 4,  
687 834–866, 10.1093/nsr/nwx150, 2017a.

688 Li, M., Zhang, Q., Zheng, B., Tong, D., Lei, Y., Liu, F., Hong, C., Kang, S., Yan, L., Zhang, Y., Bo, Y., Su,  
689 H., Cheng, Y., and He, K.: Persistent growth of anthropogenic non-methane volatile organic  
690 compound (NMVOC) emissions in China during 1990–2017: drivers, speciation and ozone  
691 formation potential, *Atmospheric Chemistry and Physics*, 19, 8897–8913, 10.5194/acp-19-8897-  
692 2019, 2019.

693 Liu, T., Wang, C., Wang, Y., Huang, L., Li, J., Xie, F., Zhang, J., and Hu, J.: Impacts of model resolution  
694 on predictions of air quality and associated health exposure in Nanjing, China, *Chemosphere*, 249,  
695 126515, 10.1016/j.chemosphere.2020.126515, 2020.

696 Liu, X., Guo, H., Zeng, L., Lyu, X., Wang, Y., Zeren, Y., Yang, J., Zhang, L., Zhao, S., Li, J., and Zhang,  
697 G.: Photochemical ozone pollution in five Chinese megacities in summer 2018, *Sci Total Environ*,  
698 801, 149603, 10.1016/j.scitotenv.2021.149603, 2021.

699 Liu, Y., Li, J., Ma, Y., Zhou, M., Tan, Z., Zeng, L., Lu, K., and Zhang, Y.: A review of gas-phase chemical  
700 mechanisms commonly used in atmospheric chemistry modelling, *Journal of Environmental*  
701 *Sciences*, <https://doi.org/10.1016/j.jes.2022.10.031>, 2022.

702 Luecken, D. J., Napelenok, S. L., Strum, M., Scheffe, R., and Phillips, S.: Sensitivity of Ambient  
703 Atmospheric Formaldehyde and Ozone to Precursor Species and Source Types Across the United  
704 States, *Environ Sci Technol*, 52, 4668–4675, 10.1021/acs.est.7b05509, 2018.

705 Lyu, X., Wang, N., Guo, H., Xue, L., Jiang, F., Zeren, Y., Cheng, H., Cai, Z., Han, L., and Zhou, Y.:  
706 Causes of a continuous summertime O<sub>3</sub> pollution event in Jinan, a central city in the North China  
707 Plain, *Atmospheric Chemistry and Physics*, 19, 3025–3042, 10.5194/acp-19-3025-2019, 2019.

708 Lyu, X., Guo, H., Wang, Y., Zhang, F., Nie, K., Dang, J., Liang, Z., Dong, S., Zeren, Y., Zhou, B., Gao,  
709 W., Zhao, S., and Zhang, G.: Hazardous volatile organic compounds in ambient air of China,  
710 *Chemosphere*, 246, 125731, 10.1016/j.chemosphere.2019.125731, 2020.

711 Ma, M., Gao, Y., Ding, A., Su, H., Liao, H., Wang, S., Wang, X., Zhao, B., Zhang, S., Fu, P., Guenther,  
712 A. B., Wang, M., Li, S., Chu, B., Yao, X., and Gao, H.: Development and Assessment of a High-  
713 Resolution Biogenic Emission Inventory from Urban Green Spaces in China, *Environ Sci Technol*,  
714 56, 175–184, 10.1021/acs.est.1c06170, 2021.

715 Ma, W., Feng, Z., Zhan, J., Liu, Y., Liu, P., Liu, C., Ma, Q., Yang, K., Wang, Y., He, H., Kulmala, M., Mu,  
716 Y., and Liu, J.: Influence of photochemical loss of volatile organic compounds on understanding  
717 ozone formation mechanism, *Atmospheric Chemistry and Physics*, 22, 4841–4851, 10.5194/acp-  
718 22-4841-2022, 2022b.

719 Mao, J., Li, L., Li, J., Sulaymon, I. D., Xiong, K., Wang, K., Zhu, J., Chen, G., Ye, F., Zhang, N., Qin, Y.,  
720 Qin, M., and Hu, J.: Evaluation of Long-Term Modeling Fine Particulate Matter and Ozone in China  
721 During 2013–2019, *Frontiers in Environmental Science*, 10, 10.3389/fenvs.2022.872249, 2022.

722 McDonald, B. C., de Gouw, J. A., Gilman, J. B., Jathar, S. H., Akherati, A., Cappa, C. D., Jimenez, J. L.,  
723 Lee-Taylor, J., Hayes, P. L., McKeen, S. A., Cui, Y. Y., Kim, S.-W., Gentner, D. R., Isaacman-VanWertz,  
724 G., Goldstein, A. H., Harley, R. A., Frost, G. J., Roberts, J. M., Ryerson, T. B., and Trainer, M.: Volatile  
725 chemical products emerging as largest petrochemical source of urban organic emissions, *Science*,  
726 359, 760–764, 10.1126/science.aaq0524, 2018.

727 Parrish, D. D., Ryerson, T. B., Mellqvist, J., Johansson, J., Fried, A., Richter, D., Walega, J. G.,  
728 Washenfelder, R. A., de Gouw, J. A., Peischl, J., Aikin, K. C., McKeen, S. A., Frost, G. J., Fehsenfeld, F.  
729 C., and Herndon, S. C.: Primary and secondary sources of formaldehyde in urban atmospheres:  
730 Houston Texas region, *Atmospheric Chemistry and Physics*, 12, 3273–3288, 10.5194/acp-12-  
731 3273-2012, 2012.

732 Peng, Y., Wang, H., Wang, Q., Jing, S., An, J., Gao, Y., Huang, C., Yan, R., Dai, H., Cheng, T., Zhang,

733 Q., Li, M., Hu, J., Shi, Z., Li, L., Lou, S., Tao, S., Hu, Q., Lu, J., and Chen, C.: Observation-based sources  
734 evolution of non-methane hydrocarbons (NMHCs) in a megacity of China, *J Environ Sci (China)*,  
735 124, 794-805, 10.1016/j.jes.2022.01.040, 2023.

736 Qin, M., Hu, A., Mao, J., Li, X., Sheng, L., Sun, J., Li, J., Wang, X., Zhang, Y., and Hu, J.: PM<sub>2.5</sub> and  
737 O<sub>3</sub> relationships affected by the atmospheric oxidizing capacity in the Yangtze River Delta, China,  
738 *Sci Total Environ*, 810, 152268, 10.1016/j.scitotenv.2021.152268, 2022.

739 Qin, M., Hu, Y., Wang, X., Vasilakos, P., Boyd, C. M., Xu, L., Song, Y., Ng, N. L., Nenes, A., and Russell,  
740 A. G.: Modeling biogenic secondary organic aerosol (BSOA) formation from monoterpene  
741 reactions with NO<sub>3</sub>: A case study of the SOAS campaign using CMAQ, *Atmospheric Environment*,  
742 184, 146-155, 10.1016/j.atmosenv.2018.03.042, 2018.

743 Sha, Q., Zhu, M., Huang, H., Wang, Y., Huang, Z., Zhang, X., Tang, M., Lu, M., Chen, C., Shi, B., Chen,  
744 Z., Wu, L., Zhong, Z., Li, C., Xu, Y., Yu, F., Jia, G., Liao, S., Cui, X., Liu, J., and Zheng, J.: A newly  
745 integrated dataset of volatile organic compounds (VOCs) source profiles and implications for the  
746 future development of VOCs profiles in China, *Sci Total Environ*, 793, 148348,  
747 10.1016/j.scitotenv.2021.148348, 2021.

748 Shao, M., Wang, B., Lu, S., Yuan, B., and Wang, M.: Effects of Beijing Olympics Control Measures  
749 on Reducing Reactive Hydrocarbon Species, *Environ. Sci. Technol.*, 45, 514-519, 2011.

750 Shao, M., Zhang, Y., Zeng, L., Tang, X., Zhang, J., Zhong, L., and Wang, B.: Ground-level ozone in  
751 the Pearl River Delta and the roles of VOC and NO<sub>x</sub> in its production, *Journal of Environmental*  
752 *Management*, 90, 512-518, 10.1016/j.jenvman.2007.12.008, 2009.

753 Shao, P., Xu, X., Zhang, X., Xu, J., Wang, Y., and Ma, Z.: Impact of volatile organic compounds and  
754 photochemical activities on particulate matters during a high ozone episode at urban, suburb and  
755 regional background stations in Beijing, *Atmospheric Environment*, 236,  
756 10.1016/j.atmosenv.2020.117629, 2020.

757 Shi, Z., Li, J., Huang, L., Wang, P., Wu, L., Ying, Q., Zhang, H., Lu, L., Liu, X., Liao, H., and Hu, J.:  
758 Source apportionment of fine particulate matter in China in 2013 using a source-oriented chemical  
759 transport model, *Sci Total Environ*, 601-602, 1476-1487, 10.1016/j.scitotenv.2017.06.019, 2017.

760 Sillman, S.: The relation between ozone, NO<sub>x</sub> and hydrocarbons in urban and polluted rural  
761 environments, *Atmos. Environ.*, 33 1821-1845, 10.1016/S1352-2310(98)00345-8, 1999.

762 Simpson, I. J., Blake, N. J., Barletta, B., Diskin, G. S., Fuelberg, H. E., Gorham, K., Huey, L. G., Meinardi,  
763 S., Rowland, F. S., Vay, S. A., Weinheimer, A. J., Yang, M., and Blake, D. R.: Characterization of trace  
764 gases measured over Alberta oil sands mining operations: 76 speciated C<sub>2</sub>-C<sub>10</sub> volatile organic  
765 compounds (VOCs), CO<sub>2</sub>, CH<sub>4</sub>, CO, NO, NO<sub>2</sub>, NO<sub>y</sub>, O<sub>3</sub> and SO<sub>2</sub>, *Atmospheric Chemistry and Physics*,  
766 10, 11931-11954, 10.5194/acp-10-11931-2010, 2010.

767 Wang, G., Zhao, N., Zhang, H., Li, G., and Xin, G.: Spatiotemporal Distributions of Ambient Volatile  
768 Organic Compounds in China: Characteristics and Sources, *Aerosol and Air Quality Research*, 22,  
769 10.4209/aaqr.210379, 2022a.

770 Wang, H., Ma, X., Tan, Z., Wang, H., Chen, X., Chen, S., Gao, Y., Liu, Y., Liu, Y., Yang, X., Yuan, B.,  
771 Zeng, L., Huang, C., Lu, K., and Zhang, Y.: Anthropogenic monoterpenes aggravating ozone  
772 pollution, *National Science Review*, 9, 10.1093/nsr/nwac103, 2022b.

773 Wang, H., Yan, R., Xu, T., Wang, Y., Wang, Q., Zhang, T., An, J., Huang, C., Gao, Y., Gao, Y., Li, X.,  
774 Yu, C., Jing, S., Qiao, L., Lou, S., Tao, S., and Li, Y.: Observation Constrained Aromatic Emissions in  
775 Shanghai, China, *Journal of Geophysical Research: Atmospheres*, 125, 10.1029/2019jd031815,  
776 2020.

777 Wang, X., Yin, S., Zhang, R., Yuan, M., and Ying, Q.: Assessment of summertime O<sub>3</sub> formation and  
778 the O<sub>3</sub>-NO<sub>x</sub>-VOC sensitivity in Zhengzhou, China using an observation-based model, *Sci Total*  
779 *Environ*, 813, 152449, 10.1016/j.scitotenv.2021.152449, 2022c.

780 Wang, X., Li, L., Gong, K., Mao, J., Hu, J., Li, J., Liu, Z., Liao, H., Qiu, W., Yu, Y., Dong, H., Guo, S., Hu,  
781 M., Zeng, L., and Zhang, Y.: Modelling air quality during the EXPLORE-YRD campaign – Part I.  
782 Model performance evaluation and impacts of meteorological inputs and grid resolutions,  
783 *Atmospheric Environment*, 246, 10.1016/j.atmosenv.2020.118131, 2021.

784 Wei, C.-B., Yu, G.-H., Cao, L.-M., Han, H.-X., Xia, S.-Y., and Huang, X.-F.: Tempo-spatial variation  
785 and source apportionment of atmospheric formaldehyde in the Pearl River Delta, China,  
786 *Atmospheric Environment*, 312, 10.1016/j.atmosenv.2023.120016, 2023.

787 Wittrock, F., Richter, A., Oetjen, H., Burrows, J. P., Kanakidou, M., Myriokefalitakis, S., Volkamer, R.,  
788 Beirle, S., Platt, U., and Wagner, T.: Simultaneous global observations of glyoxal and formaldehyde  
789 from space, *Geophysical Research Letters*, 33, 10.1029/2006gl026310, 2006.

790 Wu, R., Zhao, Y., Xia, S., Hu, W., Xie, F., Zhang, Y., Sun, J., Yu, H., An, J., and Wang, Y.: Reconciling  
791 the bottom-up methodology and ground measurement constraints to improve the city-scale  
792 NMVOCs emission inventory: A case study of Nanjing, China, *Science of The Total Environment*,  
793 812, 10.1016/j.scitotenv.2021.152447, 2022.

794 Wu, Y., Huo, J., Yang, G., Wang, Y., Wang, L., Wu, S., Yao, L., Fu, Q., and Wang, L.: Measurement  
795 report: Production and loss of atmospheric formaldehyde at a suburban site of Shanghai in  
796 summertime, *Atmospheric Chemistry and Physics*, 23, 2997-3014, 10.5194/acp-23-2997-2023,  
797 2023.

798 Xiong, C., Wang, N., Zhou, L., Yang, F., Qiu, Y., Chen, J., Han, L., and Li, J.: Component characteristics  
799 and source apportionment of volatile organic compounds during summer and winter in downtown  
800 Chengdu, southwest China, *Atmospheric Environment*, 258, 10.1016/j.atmosenv.2021.118485,  
801 2021.

802 Yang, Y., Liu, B., Hua, J., Yang, T., Dai, Q., Wu, J., Feng, Y., and Hopke, P. K.: Global review of source  
803 apportionment of volatile organic compounds based on highly time-resolved data from 2015 to  
804 2021, *Environ Int*, 165, 107330, 10.1016/j.envint.2022.107330, 2022.

805 Zhang, G., Wang, N., Jiang, X., and Zhao, Y.: Characterization of Ambient Volatile Organic  
806 Compounds (VOCs) in the Area Adjacent to a Petroleum Refinery in Jinan, China, *Aerosol and Air  
807 Quality Research*, 17, 944-950, 10.4209/aaqr.2016.07.0303, 2017.

808 Zhang, M., Zhao, C., Yang, Y., Du, Q., Shen, Y., Lin, S., Gu, D., Su, W., and Liu, C.: Modeling  
809 sensitivities of BVOCs to different versions of MEGAN emission schemes in WRF-Chem (v3.6) and  
810 its impacts over eastern China, *Geoscientific Model Development*, 14, 6155-6175, 10.5194/gmd-  
811 14-6155-2021, 2021.

812 Zhang, Q., Streets, D. G., Carmichael, G. R., He, K. B., Huo, H., Kannari, A., Klimont, Z., Park, I. S.,  
813 Reddy, S., Fu, J. S. J. A. c., and physics: Asian emissions in 2006 for the NASA INTEX-B mission,  
814 *Atmos. Chem. Phys.*, 9, 5131-5153, 10.5194/acp-9-5131-2009, 2009.

815 Zhao, M., Zhang, Y., Pei, C., Chen, T., Mu, J., Liu, Y., Wang, Y., Wang, W., and Xue, L.: Worsening  
816 ozone air pollution with reduced NO<sub>x</sub> and VOCs in the Pearl River Delta region in autumn 2019:  
817 Implications for national control policy in China, *J Environ Manage*, 324, 116327,  
818 10.1016/j.jenvman.2022.116327, 2022.

819 Zheng, B., Cheng, J., Geng, G., Wang, X., Li, M., Shi, Q., Qi, J., Lei, Y., Zhang, Q., and He, K.: Mapping  
820 anthropogenic emissions in China at 1 km spatial resolution and its application in air quality  
821 modeling, *Sci Bull (Beijing)*, 66, 612-620, 10.1016/j.scib.2020.12.008, 2021.

822 Zhou, B., Guo, H., Zeren, Y., Wang, Y., Lyu, X., Wang, B., and Wang, H.: An Observational Constraint  
823 of VOC Emissions for Air Quality Modeling Study in the Pearl River Delta Region, *Journal of  
824 Geophysical Research: Atmospheres*, 128, 10.1029/2022jd038122, 2023.

825 Zhu, S., Kinnon, M. M., Shaffer, B. P., Samuelsen, G. S., Brouwer, J., and Dabdub, D.: An uncertainty  
826 for clean air: Air quality modeling implications of underestimating VOC emissions in urban  
827 inventories, *Atmospheric Environment*, 211, 256-267, 10.1016/j.atmosenv.2019.05.019, 2019.

828

829 Table 1. Mean, median, maximum (max), minimum (min), and standard deviation (std)  
 830 of the Ratios and differences (Diff) for five VOCs groups and TVOCs at 28 sites

		Alkanes	Alkenes	Aromatics	ARO2MN (Aromatics)	Alkynes	HCHO	TVOCs
Ratio(pre/obs)	mean	0.59	0.60	1.33	0.40	0.55	1.66	0.70
	median	0.53	0.51	1.30	0.31	0.41	1.21	0.74
	max	1.87	2.46	3.29	1.96	2.36	8.70	1.90
	min	0.13	0.09	0.10	0.05	0.09	0.25	0.15
	std	0.38	0.48	0.89	0.38	0.47	1.61	0.40
	mean	-6.18	-4.02	0.42	-0.28	-1.16	0.16	-10.78
Diff(pre-obs)	median	-5.65	-2.56	0.83	-0.25	-1.04	0.49	-7.57
	max	14.12	3.50	6.09	0.24	0.87	5.57	29.53
	min	-19.40	-15.50	-8.18	-0.74	-2.64	-8.90	-50.61
	std	6.81	4.69	3.47	0.20	0.97	2.99	16.11

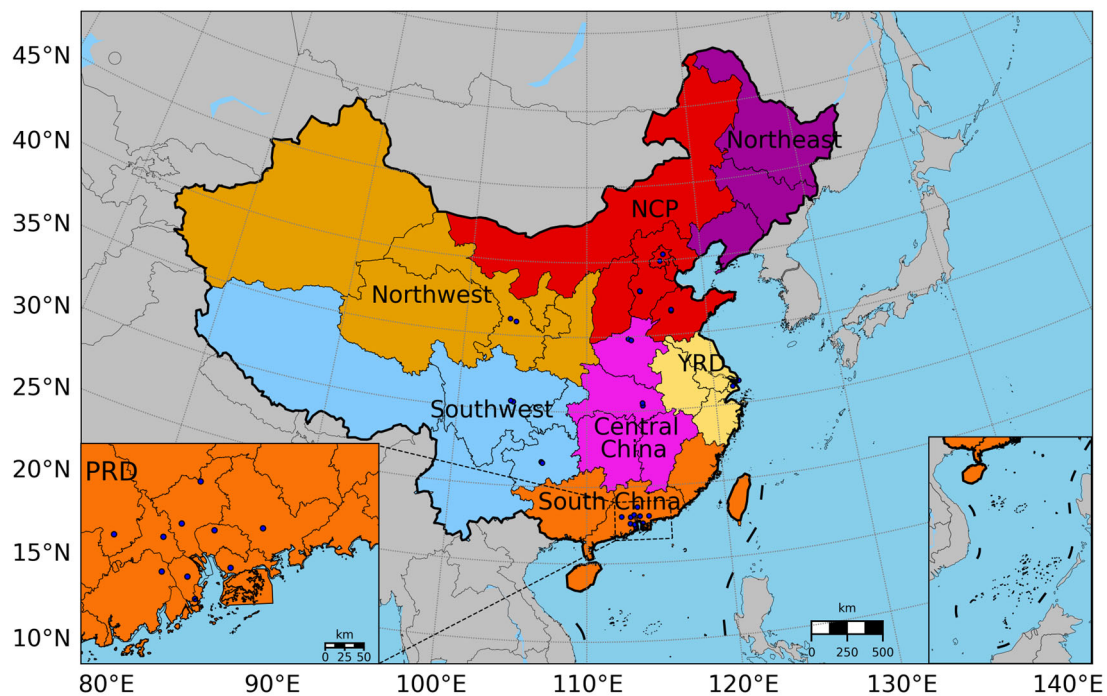
831

832

833 Table 2. New cases of adjusting emission coefficient under observation constraints

Cases in CMAQ	Changing species in MEIC	Adjusted coefficient
base case	--	--
case_NO <sub>x</sub>	NO, NO <sub>2</sub>	1.5
case_ALK2	ALK2	4.6
case_ARO2MN	ARO2MN	3.2
case_BENZ	BENZ	0.4
case_OLE1	OLE1	2.0
case_PRPE	PRPE	2.1
case_ACYE	ACYE	2.8
case_all	all of the above VOCs	

834

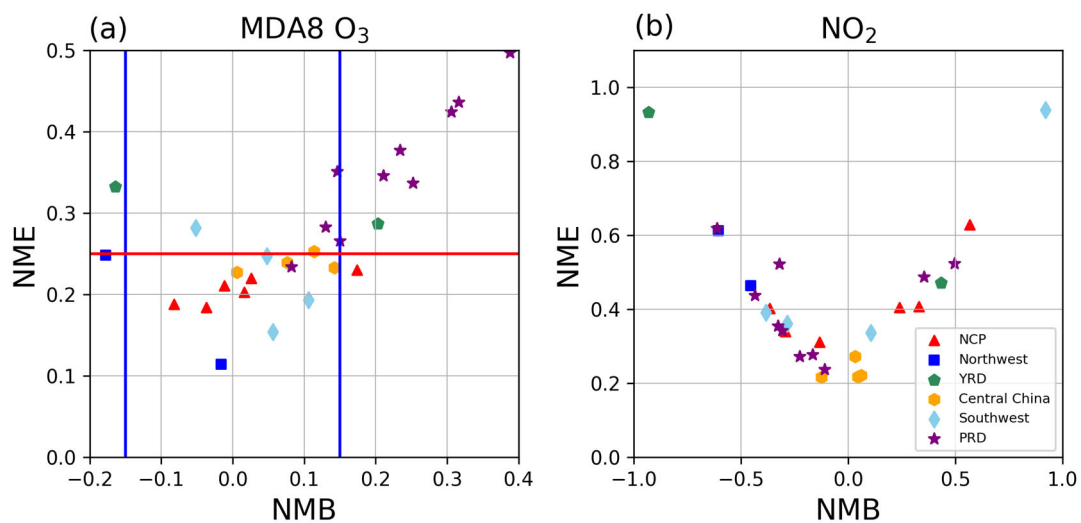


835

836 Figure 1. The CMAQ modelling domain cover China and the surrounding countries and

837 regions in this study, including 28 blue dots that represent the positions of VOCs

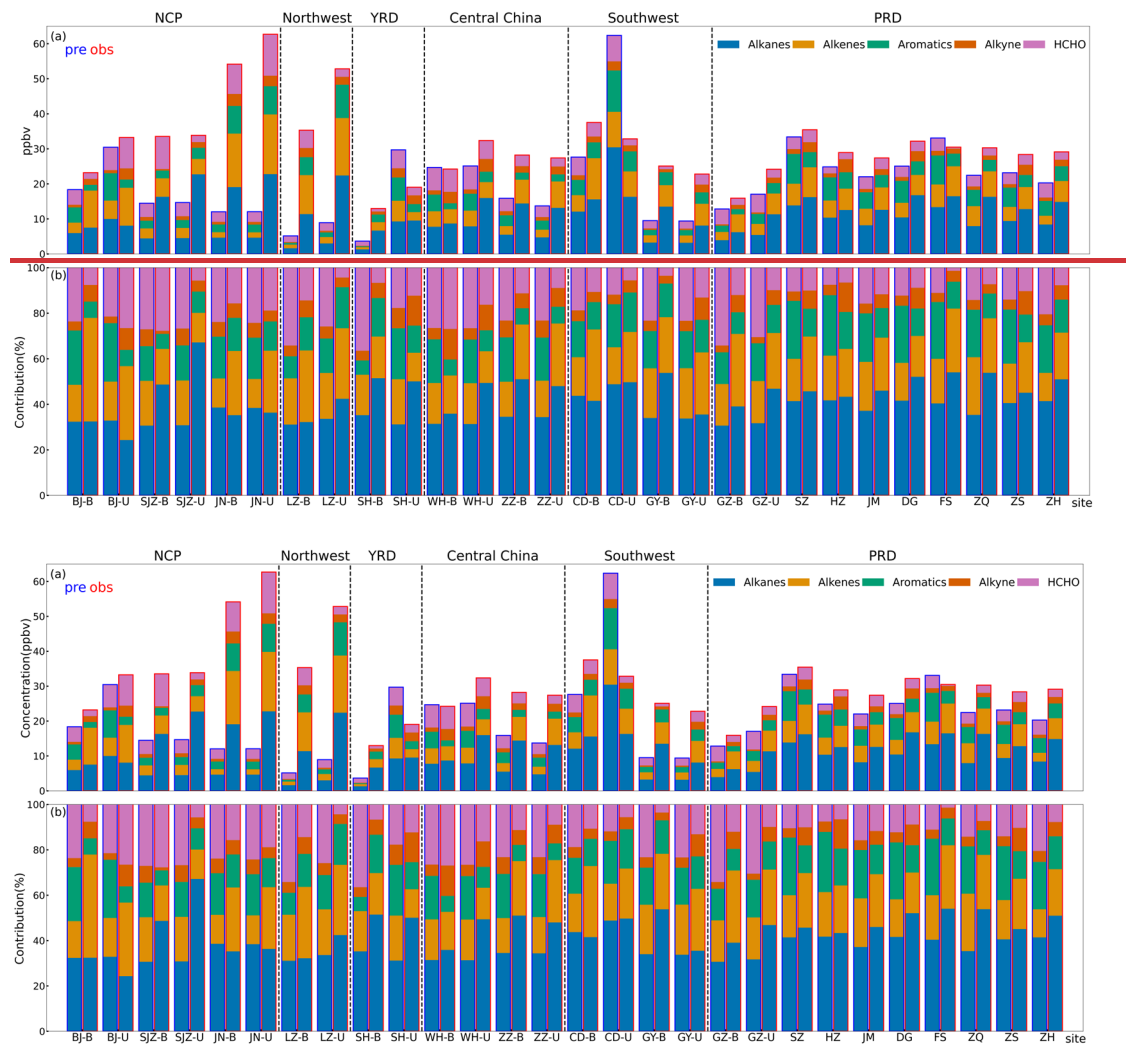
838 sampling sites. We divided China into seven regions according to the geographical  
 839 location of different provinces, which comprise the following sites: NCP: BJ-B, BJ-U,  
 840 SJZ-B, SJZ-U, JN-B, JN-U; Northwest: LZ-B, LZ-U; Northeast (nNo observation site);  
 841 YRD: SH-B, SH-U; Central China: ZZ-B, ZZ-U, WH-B, WH-U; Southwest: CD-B,  
 842 CD-U, GY-B, GY-U; South China: Most of the sites are concentrated in PRD region  
 843 (shown in the enlarged subgraph in the lower left): GZ-B, GZ-U, SZ, HZ, DG, FS, JM,  
 844 ZQ, ZS, ZH.



845

846 Figure 2. Model performance on MDA8 O<sub>3</sub> and NO<sub>2</sub> at 28 sites in different regions  
 847 from June 6th to August 24th in 2018. The blue and red lines denote performance  
 848 criteria (NMB: normalized mean bias, NME: normalized mean error) for MDA8 O<sub>3</sub>  
 849 suggested by Emery et al. (2017) and the symbols in different colors distinguish  
 850 different regions of China.

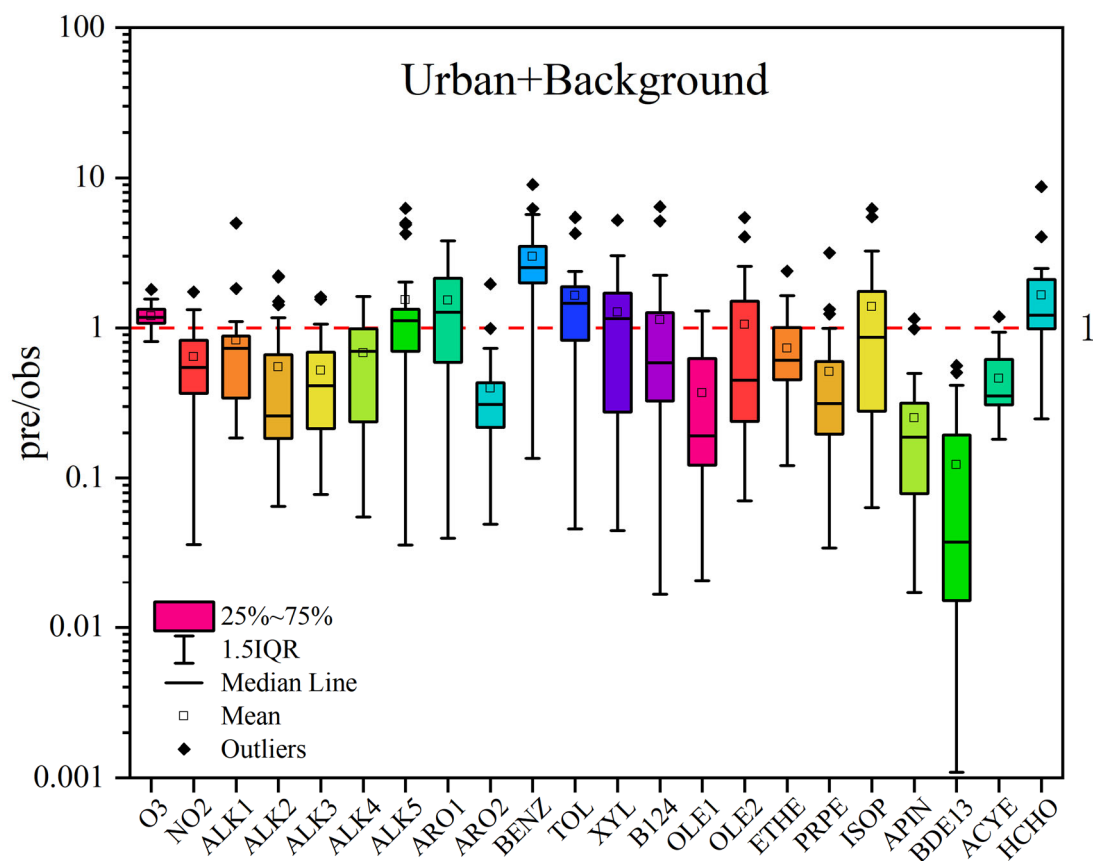




851

852

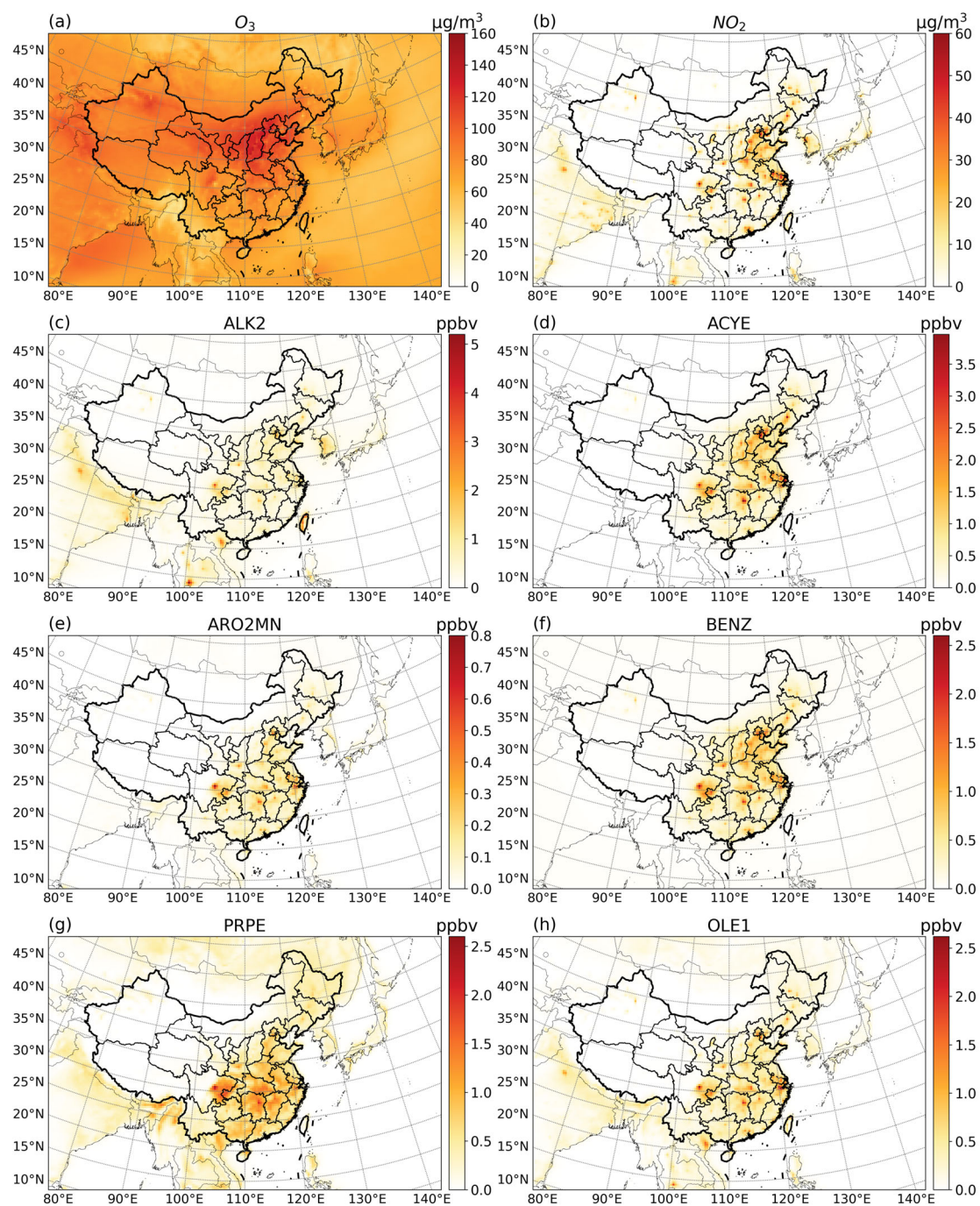
853 Figure 3. Comparison of predicted and observed VOCs at 28 sites during the study  
 854 period. (a) The predicted (bars outlined in blue) and observed (bars outlined in red)  
 855 concentrations at each site; (b) same as (a) but with contributions of VOC  
 856 groups. Comparison of predicted and observed VOCs at 28 sites during the study period.  
 857 (a) The concentration of VOCs, for each site, on the left are prediction values with a  
 858 blue edge, and on the right are observation values with a red edge; (b) Percentage of  
 859 VOCs.



860

861 Figure 4. The ratios of prediction-to-observation (pre/obs) for O<sub>3</sub>, NO<sub>2</sub> and individual  
 862 VOCs at 28 sites (including urban and background). The horizontal midlines in boxes  
 863 represent the median values and the hollow squares depict the mean values. The boxes  
 864 represent the ratios ranging from the lower and upper quartile for individual VOCs at  
 865 all sites, and the whiskers represent the 1.5 Interquartile Range (1.5 IQR).The  
 866 predicted/observed ratio (pre/obs) of O<sub>3</sub>, NO<sub>2</sub> and different VOCs species at 28 sites  
 867 (both urban and background). The rectangles with different colors represent the ratio  
 868 range of 25% to 75% for all sites. The vertical lines with a horizontal bar are called 1.5  
 869 Interquartile Range (1.5 IQR). The horizontal lines in rectangles represent the median  
 870 value and the hollow dots are the mean value. The dots outside the 1.5 IQR are Outliers.

871



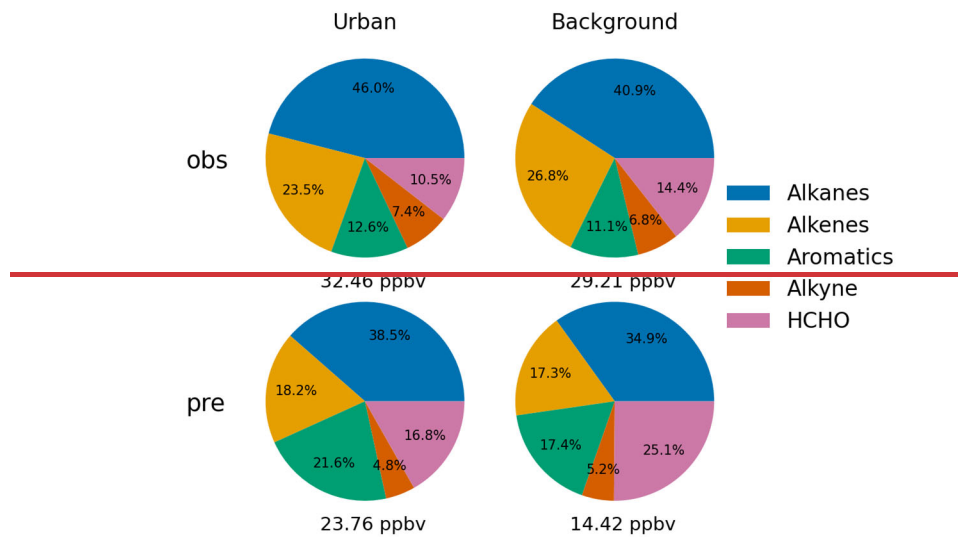
872

873 Figure 5. Predicted Prediction concentration of (a)  $O_3$ , (b)  $NO_2$  and (c-h) six VOCs

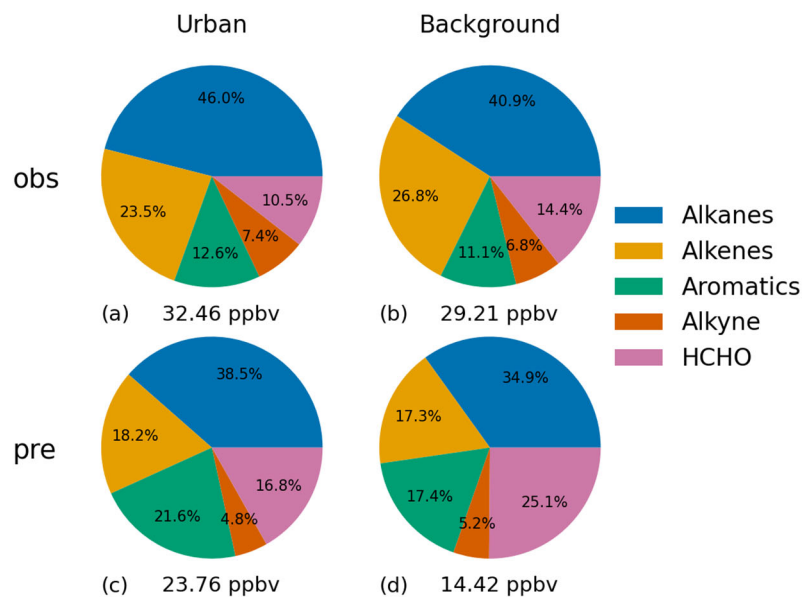
874 species in the base case from June 6th to August 24th in 2018.

875

876



877



878 Figure 6. Observed and predicted contributions of different VOCs to the total VOC  
879 concentrations at (a and c) urban sites and (b and d) background sites. Observed and  
880 predicted values of different VOCs species by sites average.